Systematic noise analysis of CAPD based time-of flight cameras

T. Van den Hauwe, W. van der Tempel, R. Grootjans,
D. Van Nieuwenhove and Maarten Kuijk

Vrije Universiteit Brussel, Electronics and Informatics Department ETRO (LAMI), Pleinlaan 2, 1050 Brussels, Belgium

A study on a new ranging camera operating on the Time-of-Flight principle using 870nm active illumination is presented. The key component of this camera is a sensor comprised of 120x90 pixels based on a Current Assisted Photonic Demodulator (CAPD), implemented in standard CMOS 0.35μm technology. The resulting camera system is capable of providing real-time accurate depth maps of the scene. An analysis was performed of the systematic noise of obtained depth map under various conditions. Measurement results with different modulation frequencies are presented showing non-linearities over the frequency range. In conclusion a compensation technique is proposed.

Introduction

Machine vision has seen interesting advances in the past years, especially with the advent of new range finding solutions. These new techniques allow machines to see the world in three dimensions in real-time and have opened the door to a wide range of new applications in areas such as robotics, medical imaging, industrial inspection and the automotive sector.

Many of these systems are based on the Time-of-Flight (TOF) principle [1]. A light source is used to emit a modulated optical signal. This light is reflected by the scene and captured by a detector. Finally, the received reflected optical signal is correlated with the electrical source signal, and the phase shift between the emitted and received signal is obtained. Using the speed of light and the modulation frequency, a distance is calculated from this phase shift.

A powerful device, which detects the incoming light and performs the demodulation at the substrate level, is the *Current Assisted Photonic Demodulator* (CAPD), described in [2] and [3].

Definitions

To obtain an unambiguous phase shift between 0 and 360 degrees, at least two measurements are required: the received reflected optical signal correlated with the original and with a 90 degrees phase-shifted version of the original. In practice, 4 measurements are used to eliminate offsets inside of each pixel, namely correlations with the signal phase-shifted over 0, 90, 180 and 270 degrees. The resulting measurements we call $V_{0°}$, $V_{90°}$, $V_{180°}$ and $V_{270°}$. The in-phase (I) and quadrature (Q) information are then defined by Eq 1.

$$I = V_{0°} - V_{180°}$$
$$Q = V_{90°} - V_{270°} \qquad \text{Eq 1}$$

$$N = |I| + |Q| \qquad \text{Eq 2}$$

We also define the norm N as the L^1 norm of a point in the I-Q plane. It is a measure of TOF signal strength and its formula is given in Eq 2.

Camera System

The camera system under study is composed of a 120x90 pixel sensor, based on the aforementioned CAPD device. The illumination module consists of an LED array which emits 870nm near infrared (NIR) light.
In the rest of this paper we will take a closer look at two sources of systematic noise in this camera system: one that is caused by limitations at the sensor level and one caused by system design.

Systematic Noise at Sensor Level

Systematic noise stemming from the CAPD device is primarily introduced by the limited bandwidth of the device. Fig 1 shows measurements, whereby the X- and Y-axis represent the in-phase (I) and quadrature (Q) measurement, respectively. For square-wave modulation, the plot should have a diamond shape, for sinusoidal modulation it should have a circular shape. It can be seen that towards higher frequencies, the measurements converge from a diamond shape to a circle, because the higher harmonics of the square-wave base frequency fall outside of the device's bandwidth.

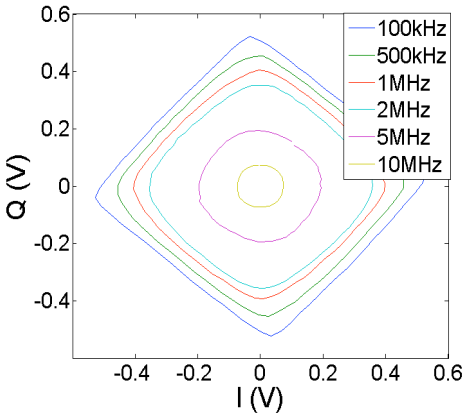

Fig 1 I-Q plot of a CAPD device. For low frequencies, the plot is diamond-shaped. For higher frequencies, the plot converges to a circle [2].

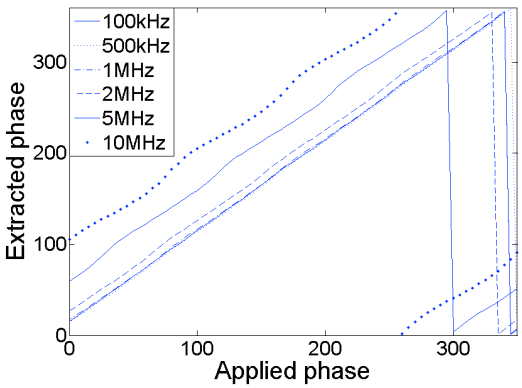

Fig 2 Measured versus applied phase shift of an optical signal [2].

To obtain the phase, Eq 3 can be used for square modulation, and Eq 4 for sinusoidal modulation. Because at the used modulation frequency, the shape is neither a diamond, nor a circle, neither of both equations is free of systematic error.

$$\phi_{square} \sim \frac{Q}{|I|+|Q|} \qquad \text{Eq 3}$$

$$\phi_{sine} = \arctan\left(\frac{Q}{I}\right) \qquad \text{Eq 4}$$

Using Eq 3, Fig 2 was constructed: it depicts the measured phase shift vs. the optically applied phase shift. It is clear from this figure that the limited device bandwidth gives rise to a systematic periodic error, on top of a constant frequency-dependent offset.

Systematic Noise at System Level

Measurements of the complete camera system were done on a checkerboard pattern. Measurements were taken at 2 different integration times: 100 and 400 microseconds, and were averaged over 100 frames to reduce the stochastic noise.

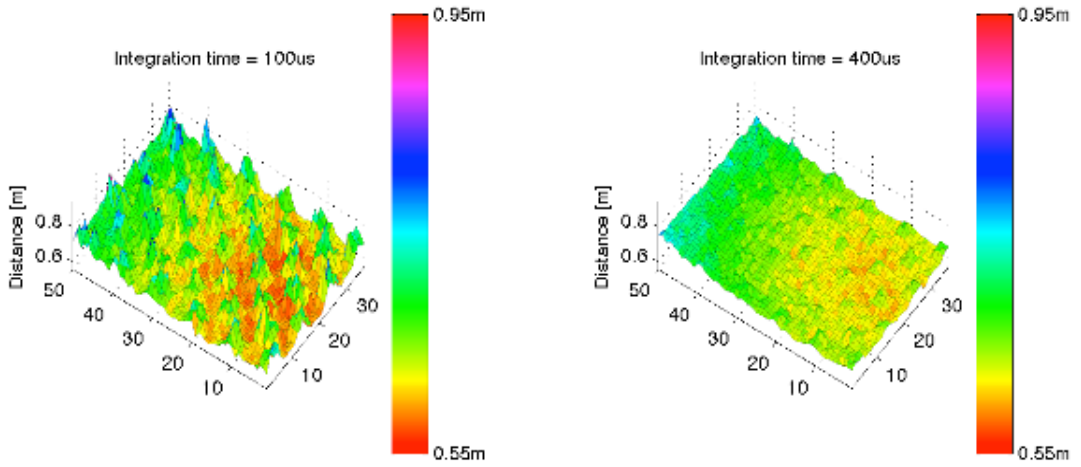

Fig 3 Depth map of the checkerboard pattern for integration times of 100µs (left) and 400µs (right)

In Fig 3, the measured depth maps are shown. The different signal strengths caused by the checkerboard clearly influence the depth measure. Low-reflectivity of the measured object causes it to appear further away from the camera. The difference in distance between low-reflectivity and high-reflectivity targets decreases as the TOF signal strength increases, as shown by the smaller peaks in the right image of Fig 3.

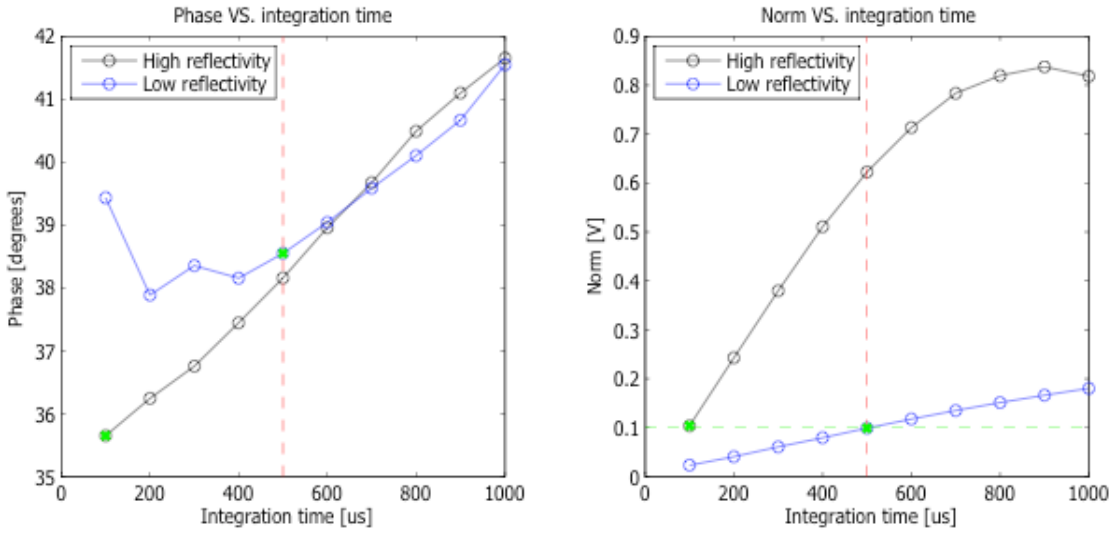

Fig 4 Measured distance (left) and norm (right) vs. integration time for high- and low-reflectivity targets averaged over 1000 measurement cycles

One also notices that the high-reflectivity squares are measured to be closer by in the left image of Fig 3 than in the right image. At first glance, this seems to contradict the previous statement that low signal strength causes an object to appear further away, since the left image has lower overall signal strength because of the shorter integration time. However, the varying signal strength is induced differently for both cases, explaining the different behaviour.

To quantify both contributions, a white, high reflectivity, and a black, low reflectivity square of the checkerboard were each measured over 1000 frames in the 4 centre pixels of the TOF camera. The averaged results were presented in Fig 4.

The right plot of Fig 4 shows a linear relation between norm and integration time. The deviation from the linear curve on the right of the dashed red line indicates saturation of the sensor. In this region the resulting calculated phase will also be erroneous. Therefore the sensor data should only be considered up to an integration time of 500µs.
The left plot of Fig 4 indicates a linear dependence of phase offset on integration time for the high reflectivity target. In this measurement set, for the low-reflectivity target, the behaviour appeared to be different, but tough to fit to a curve. The difference between these relations causes the relative systematic errors for both reflectivities.
As the phase offset for both measurements marked in green in Fig 4 have the same norm but a different phase, we can also conclude that at least two variables influence this non-linear behaviour.

Look-up Table

The systematic errors discussed in this paper could possibly be eliminated by using a look-up table (LUT). Our measurements have shown that there are at least three different contributions to these systematic errors: modulation frequency, integration time and modulated light power. Possible other influential factors include absolute distance to the target and pixel non-uniformity. Because a high-dimensional LUT would take too much storage space and calibration time, we propose to split the phase offset into contributions caused by one or two of the aforementioned variables and use multiple one-dimensional LUTs.
Additional research and more precise measurements are needed to identify all variables that influence the phase offset and to construct the proposed LUTs. This is part of the future work.

Conclusion

A 120x90 pixel Time-of-Flight camera, using a sensor based on the Current Assisted Photonic Demodulator was presented. Measurements on both sensor and system showed a dependency of the measured phase shift on both modulation frequency and signal strength. It was concluded that these dependencies could possibly be cancelled by using multiple look-up tables, but additional research is needed to implement such tables.

Acknowledgements

T. Van den Hauwe and R. Grootjans are indebted to the Institute for the Promotion of Innovation through Science and Technology in Flanders (IWT-Vlaanderen) for the financial support.

References

[1] Hosticka, B., Seitz, P., Simoni, A., “Optical Time-of-Flight Sensors for Solid-State 3D-Vision”, Encyclopedia of sensors, 2005.

[2] W. Van der Tempel, D. Van Nieuwenhove, R. Grootjans and M. Kuijk, “Lock-in pixel using a Current assisted photonic demodulator Implemented in 0.6µm Standard CMOS”, Japanese Journal of Applied Physics, Vol. 46, No. 4B, 2007.

[3] D. Van Nieuwenhove, W. van der Tempel, R. Grootjans, J. Stiens, and M. Kuijk. “Photonic demodulator with sensitivity control”, Sensors Journal, IEEE, 7(3):317–318, March 2007.